Collective circular motion of multi-vehicle systems ⋆

N. Ceccarelli [a] M. Di Marco [a] A. Garulli [a], A. Giannitrapani [a]

[a] *Dipartimento di Ingegneria dell'Informazione, Università di Siena*

Abstract

This paper addresses a collective motion problem for a multi-agent system composed of nonholonomic vehicles. The aim of the vehicles is to achieve circular motion around a virtual reference beacon. A control law is proposed, which guarantees global asymptotic stability of the circular motion with a prescribed direction of rotation, in the case of a single vehicle. Equilibrium configurations of the multi-vehicle system are studied and sufficient conditions for their local stability are given, in terms of the control law design parameters. Practical issues related to sensory limitations are taken into account. The transient behavior of the multi-vehicle system is analyzed via numerical simulations.

Key words: Multi-agent systems, nonholonomic vehicles, collective motion, stability.

1 Introduction

Multi-agent systems have received increased interest in recent years, due to their enormous potential in several fields: collective motion of autonomous vehicles, exploration of unknown environments, surveillance, distributed sensor networks, biology, etc. (see e.g. (Jadbabaie *et al.*, 2003; Marshall *et al.*, 2004) and the references therein). Starting from the seminal works by Reynolds (1987) and Vicsek *et al.* (1995), several theoretical frameworks have been proposed to analyze the collective motion of multi-agent systems. A typical aim of these approaches is to formulate decentralized control laws driving the team of agents to pre-specified equilibrium configurations.

Although a rigorous stability analysis of multi-agent systems is generally a very difficult task, nice theoretical results have been obtained in the case of linear models. One of the first contributions in this respect was given in (Leonard and Fiorelli, 2001), where a multi-vehicle system with a virtual reference beacon is considered. Parallel and circular motions are obtained by applying a control law based on artificial potentials and stability is proven via Lyapunov arguments. Leader following and leaderless coordination problems have been studied in (Jadbabaie *et al.*, 2003; Lin *et al.*, 2004). In particular, in (Jadbabaie *et al.*, 2003) sufficient conditions are given for convergence of the Vicsek's control scheme, by explicitly taking into account the time-varying topology of the multi-agent system. More complex local control laws, based on the combination of attractive, repulsive and alignment forces, have been proposed in (Tanner *et al.*, 2007). Stability of collective parallel motion is achieved, while ensuring collision avoidance among the agents. An approach for the analysis of multi-agent systems, based on partial difference equation over graphs, has been proposed in (Ferrari-Trecate *et al.*, 2006). General frameworks for dealing with consensus problems in linear and nonlinear settings have been presented in (Olfati-Saber and Murray, 2004; Xiao and Boyd, 2004; Moreau, 2005). These works study in depth how the topology of the communication network affects the behavior of the multi-agent system.

Stability analysis becomes more challenging when kinematic constraints are taken into account, as in the case of wheeled nonholonomic vehicles. Unicycle-like motion models have been recently considered in several papers. In (Justh and Krishnaprasad, 2004; Paley *et al.*, 2004) different control laws are proposed for circular and parallel motion of planar multi-vehicle systems. A complete stability analysis of the two-vehicle case, and of the circular motion of a single-vehicle around a fixed beacon, is given in (Justh and Krishnaprasad, 2004). Moreover, it is shown that for a wide class of control laws, the general n-vehicle system admits only two sets of equilibrium configurations, corresponding to parallel and circular motion. Two different control laws stabilizing collective motion in parallel and circular configurations are presented in (Paley *et al.*, 2004). A possible drawback of the above control schemes is that both clockwise and counterclockwise rotations are stabilized. In (Sepulchre *et al.*, 2007), a family of controllers, stabilizing different collective patterns, is presented. The proposed control laws depend on the relative orientation and relative spacing of the agents, and assume an all-to-all communication network. The latter assumption is relaxed in (Jeanne *et al.*, 2005), where the circular motion of particles in symmetric patterns is investigated for a ring-like coupling network. In (Marshall *et al.*, 2004), equilibrium

⋆ This paper was not presented at any IFAC meeting. N. Ceccarelli is now with Nuovo Pignone S.p.A., Firenze, Italy.

Email address: garulli@dii.unisi.it (A. Garulli).

formations of multi-vehicle systems in cyclic pursuit are studied. A simple control law is proposed allowing the vehicles to achieve circular motion configurations, whose local stability is analyzed in detail. The cyclic pursuit strategy requires the vehicles to be labelled and each vehicle must always perceive its unique neighbor, thus imposing quite strong sensory and communication requirements.

The problem considered in this paper is that of a team of nonholonomic vehicles whose objective is to achieve collective circular motion around a virtual reference beacon. As a first contribution, a control law is proposed, which is shown to guarantee global asymptotic stability of the counterclockwise circular motion around a fixed beacon, in the single-vehicle case. This turns out to be a useful property also in the multi-agent case, because all vehicles try to rotate around the beacon in the same direction of rotation. Then, the control law is suitably modified to cope with the multi-vehicle case. Equilibrium configurations of the multi-vehicle system under the proposed control law are discussed and sufficient conditions for local asymptotic stability are derived in terms of the control law design parameters. Sensory limitations are explicitly taken into account; in particular: i) each agent can perceive only vehicles lying in a limited visibility region; ii) a vehicle cannot measure the orientation of another vehicle, but only its relative position; iii) vehicles are indistinguishable. Moreover, the proposed control law is completely decentralized and information exchange between the vehicles is not required. Simulation results demonstrate the effectiveness of the proposed approach in the multi-vehicle case. Guidelines for the choice of the control law parameters are provided, taking into account the tradeoff between fast convergence to the equilibrium configuration and safe collision-free trajectories. A preliminary version of the paper has appeared in (Ceccarelli *et al.*, 2005).

The paper is organized as follows. In Section 2, the control law for the single-vehicle case is introduced. Global asymptotic stability of the counterclockwise circular motion around a fixed beacon is proved. Section 3 concerns the multi-vehicle scenario: the modified control law is presented and the resulting equilibrium configurations are studied. Sufficient conditions for local stability are given. Simulation results are provided in Section 4, along with a thorough analysis of the role of the control law design parameters. Concluding remarks and future research directions are outlined in Section 5.

2 Control law for a single vehicle

Consider the planar unicycle model

$$\dot{x}(t) = v\,\cos\theta(t) \tag{1}$$
$$\dot{y}(t) = v\,\sin\theta(t) \tag{2}$$
$$\dot{\theta}(t) = u(t); \tag{3}$$

where $[x\ y\ \theta]' \in \mathbb{R}^2 \times [-\pi, \pi)$ represents the vehicle pose, v is the forward speed (assumed to be constant) and $u(t)$ is the angular speed, which plays the role of control input.

The following control law, based on the vehicle's relative pose with respect to a reference *beacon*, is proposed

$$u(t) = \begin{cases} k \cdot g(\rho(t); c, \rho_0) \cdot \alpha_d(\gamma(t)) & \text{if } \rho(t) > 0 \\ 0 & \text{if } \rho(t) = 0 \end{cases} \tag{4}$$

with

$$g(\rho; c, \rho_0) = \ln\Big(\frac{(c-1)\cdot\rho + \rho_0}{c\cdot\rho_0}\Big) \tag{5}$$

$$\alpha_d(\gamma) = \begin{cases} \gamma & \text{if } \ 0 \le \gamma \le \psi \\ \gamma - 2\pi & \text{if } \ \psi < \gamma < 2\pi. \end{cases} \tag{6}$$

In (4)-(6), ρ is the distance between the vehicle position $\mathbf{r}_v{=}[x\ y]'$ and the beacon position $\mathbf{r}_b = [x_b\ y_b]'$; $\gamma \in [0, 2\pi)$ represents the angular distance between the heading of the vehicle and the direction of the beacon (see Figure 1); $k > 0$, $c > 1$, $\rho_0 > 0$ and $\psi \in (\frac{3}{2}\pi, 2\pi)$ are given constants.

The terms in equation (4) have the following meaning. When $\gamma \le \psi$ (and hence $\alpha_d > 0$), if $\rho > \rho_0$ the input $u(t)$ is positive and favors counterclockwise rotation of the vehicle. Conversely, if $\gamma \le \psi$ and $\rho < \rho_0$ (vehicle close to the beacon) the vehicle is steered clockwise until it is sufficiently faraway from the beacon. The threshold ψ in (6) is introduced so that, when ρ is large and γ is close to 2π, the vehicle is forced to head for the beacon without making useless circular motions. It will be shown that the choice $\psi > \frac{3}{2}\pi$ is necessary to prevent clockwise rotation about the beacon from being an equilibrium solution. In order to analyze system (1)-(6), let us exploit the representation of vectors in $\mathbb{R}^2$ via complex numbers (Justh and Krishnaprasad, 2004). Then, one can set

$$\mathbf{r} = \mathbf{r}_b - \mathbf{r}_v = \rho\, e^{i\Gamma} \tag{7}$$
$$\rho = \sqrt{(x - x_b)^2 + (y - y_b)^2} \tag{8}$$
$$\gamma = (\Gamma - \theta) \mathrm{mod}(2\pi) \tag{9}$$

where $\Gamma \in [0, 2\pi)$ denotes the angular distance between $\mathbf{r}$ and the x-axis (see Figure 1). By differentiating (7)

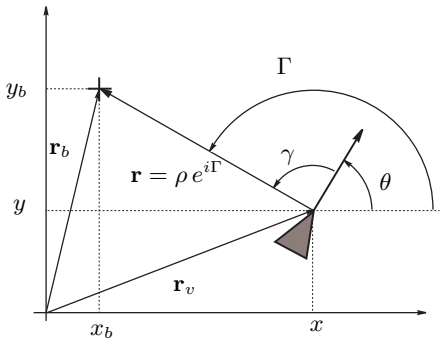

Fig. 1. Vehicle (triangle) and beacon (cross).

with respect to time, one obtains $\dot{\mathbf{r}} = \dot{\rho}\, e^{i\Gamma} + i\rho\,\dot{\Gamma} e^{i\Gamma}$. For a static beacon one has $\dot{\mathbf{r}} = -\dot{\mathbf{r}}_v = -v\, e^{i\theta} = -v\, e^{-i\gamma}\, e^{i\Gamma}$, and hence for $\rho \neq 0$

$$\dot{\rho} = -v\,\cos\gamma \tag{10}$$
$$\dot{\Gamma} = \frac{v}{\rho}\,\sin\gamma\,. \tag{11}$$

By differentiating (9) with respect to time, using (10)-(11) and (4)-(6), one obtains the system

$$\begin{aligned} \dot{\rho} &= -v\,\cos(\gamma) \\ \dot{\gamma} &= \begin{cases} \dfrac{v}{\rho}\sin\gamma - k g(\rho;c,\rho_0)\gamma & \text{if } 0 \le \gamma \le \psi \\ \dfrac{v}{\rho}\sin\gamma - k g(\rho;c,\rho_0)(\gamma - 2\pi) & \text{if } \psi < \gamma < 2\pi. \end{cases} \end{aligned} \tag{12}$$

The first aim is to show that (12) has a unique equilibrium point, corresponding to counterclockwise rotation of the vehicle around the beacon. To this end, let us select the parameters v, k, c, ρ_0 so that

$$\min_{\rho}\ \rho\, g(\rho;c,\rho_0)\ >\ -\frac{2\,v}{3\,\pi\,k}. \tag{13}$$

This choice guarantees that for $\gamma = \frac{3}{2}\pi$ one has $\dot{\gamma} < 0$ for any ρ, i.e. there are no equilibria of system (12) such that $\gamma = \frac{3}{2}\pi$, or equivalently clockwise rotation is not a limit cycle for system (1)-(6).
Let $\mathcal{D} = \mathbb{R}_{++} \times (0, 2\pi)$, where $\mathbb{R}_{++}$ denotes the set of strictly positive real numbers. The following result holds.

Proposition 1 *The point $p_e = \left[\rho_e\ \frac{\pi}{2}\right]'$ where ρ_e is such that:*

$$\frac{v}{\rho_e} - k\, g(\rho_e;c,\rho_0)\,\frac{\pi}{2} = 0 \tag{14}$$

is the only equilibrium of system (12), for $(\rho,\gamma) \in \mathcal{D}$.

From Proposition 1 one has that the counterclockwise circular motion with radius ρ_e and angular velocity $\dot{\Gamma} = \frac{v}{\rho_e}$ is a limit cycle for system (1)-(6). The rest of this section will be devoted to proving global asymptotic stability of such a limit cycle.
Let us introduce the following Lyapunov function which is instrumental in the stability analysis of the equilibrium p_e for system (12):

$$V(\rho,\gamma) = \int_{\rho_e}^{\rho} A(\hat{\rho})d\hat{\rho} + \int_{\frac{\pi}{2}}^{\gamma} B(\hat{\gamma})d\hat{\gamma} \tag{15}$$

where

$$A(\rho) = \frac{2}{\pi v}\left(k\, g(\rho;c,\rho_0)\,\frac{\pi}{2} - \frac{v}{\rho}\right) \tag{16}$$

$$B(\gamma) = \begin{cases} -\dfrac{\cos\gamma}{\gamma} & \text{if } 0 < \gamma \le \psi \\ -\dfrac{\cos\gamma}{\gamma - 2\pi} & \text{if } \psi < \gamma < 2\pi. \end{cases} \tag{17}$$

Hence

$$\dot{V}(\rho,\gamma) = \begin{cases} \dfrac{v}{\rho}\left(\dfrac{2}{\pi} - \dfrac{\sin\gamma}{\gamma}\right)\cos\gamma & \text{if } 0 < \gamma \le \psi \\ \dfrac{v}{\rho}\left(\dfrac{2}{\pi} - \dfrac{\sin\gamma}{\gamma - 2\pi}\right)\cos\gamma & \text{if } \psi < \gamma < 2\pi. \end{cases}$$

Define the following sets:

$$\bar{\mathcal{D}} = \mathbb{R}_{++} \times \left(0, \tfrac{3}{2}\pi\right],\ \hat{\mathcal{D}} = \mathcal{D} \backslash \bar{\mathcal{D}},\ \mathcal{K} = \mathbb{R}_{++} \times (\psi, 2\pi). \tag{18}$$

It can be checked that $V(\rho,\gamma) \ge 0\ \forall(\rho,\gamma)$; $\dot{V}(\rho,\gamma) \le 0$ for $(\rho,\gamma) \in \bar{\mathcal{D}}$, and $\dot{V}(\rho,\gamma) < 0$ for $(\rho,\gamma) \in \mathcal{K}$. Moreover $V(\rho,\gamma) = 0$ only for $\rho = \rho_e, \gamma = \frac{\pi}{2}$ and $V(\rho,\gamma)$ is radially unbounded on $\mathcal{D}$, i.e.

$$\lim_{\rho\to 0} V(\rho,\gamma) = +\infty \qquad \lim_{\rho\to\infty} V(\rho,\gamma) = +\infty$$
$$\lim_{\gamma\to 0} V(\rho,\gamma) = +\infty \qquad \lim_{\gamma\to 2\pi} V(\rho,\gamma) = +\infty.$$

By using the Lyapunov function (15), it is possible to prove the main result of this section.

Theorem 1 *The counterclockwise circular motion around a fixed beacon, with rotational radius ρ_e defined in (14) and angular velocity $\frac{v}{\rho_e}$, is a globally asymptotically stable limit cycle for system* (1)-(6).

In order to prove Theorem 1, two preliminary lemmas are needed. First, it is shown that for any initial condition in $\hat{\mathcal{D}}$, there exists a finite time $\bar{t}$ such that $(\rho(\bar{t}),\gamma(\bar{t})) \in \bar{\mathcal{D}}$ (Lemma 1). Then, it is proved that for initial vehicle poses outside $\mathcal{D}$ (i.e., when $\gamma = 0$ or $\rho = 0$), there exists a finite time $\hat{t}$ such that $(\rho(\hat{t}),\gamma(\hat{t})) \in \bar{\mathcal{D}}$ (Lemma 2). From these two lemmas, one can conclude that every trajectory starting outside $\bar{\mathcal{D}}$ will end up in $\bar{\mathcal{D}}$ in finite time (a phase portrait of vector field (12) is depicted in Figure 2). Finally, Theorem 1 is proved by using Lyapunov arguments in $\bar{\mathcal{D}}$.

Lemma 1 *Let $\bar{\mathcal{D}}$ and $\hat{\mathcal{D}}$ be given by* (18). *For any trajectory of system* (12) *with initial condition $(\rho(0),\gamma(0)) \in \hat{\mathcal{D}}$, there exists a finite time $\bar{t} > 0$ such that $(\rho(\bar{t}),\gamma(\bar{t})) \in \bar{\mathcal{D}}$.*

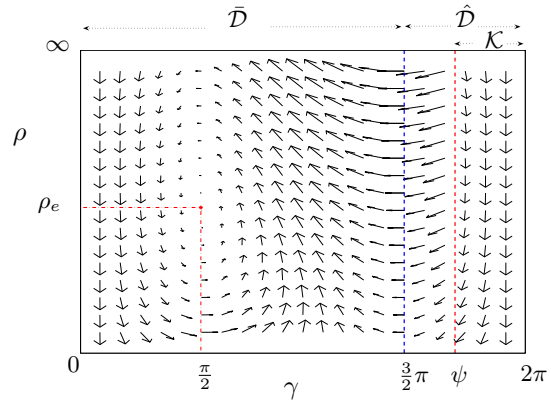

Fig. 2. Vector field (12) on $\mathcal{D}$.

Proof: See Appendix A. □
Now, let us consider all the initial vehicle poses such that the vehicle points towards the beacon, or the vehicle lies exactly on the beacon, i.e.

$$\begin{aligned}\mathcal{B} = &\{(\mathbf{r}_v(0), \theta(0)) : \gamma = 0,\ 0 < \rho < \infty\} \\ &\bigcup \{(\mathbf{r}_v(0), \theta(0)) : \rho = 0\}.\end{aligned} \tag{19}$$

Lemma 2 *Let $\bar{\mathcal{D}}$ and $\mathcal{B}$ be given by* (18) *and* (19)*, respectively. For any trajectory of system* (1)-(6) *with initial conditions in $\mathcal{B}$, there exists a finite time $\hat{t}$ such that $(\rho(\hat{t}), \gamma(\hat{t})) \in \bar{\mathcal{D}}$.*

Proof: See Appendix B. □
Now Theorem 1 can be proved.
Proof of Theorem 1: From Lemmas 1 and 2 it follows that for any initial condition $(\mathbf{r}_v(0), \theta(0)) \in \mathbb{R}^2 \times [0, 2\pi)$, there exists a finite time $t^* \geq 0$ such that $(\rho(t^*), \gamma(t^*)) \in \bar{\mathcal{D}}$. We want to prove that any trajectory of (12) starting in $\bar{\mathcal{D}}$ converges to the equilibrium p_e defined in Proposition 1. Notice that in $\bar{\mathcal{D}}$ system (12) boils down to

$$\begin{aligned}\dot{\rho} &= -v \cos\gamma \\ \dot{\gamma} &= \frac{v}{\rho} \sin\gamma - k\, g(\rho; c, \rho_0)\, \gamma.\end{aligned} \tag{20}$$

Consider any initial condition $(\rho(0), \gamma(0)) \in \bar{\mathcal{D}}$. Define $\eta = V(\rho(0), \gamma(0))$ and $\mathcal{S}_\eta = \left\{(\rho, \gamma) \in \bar{D} : V(\rho, \gamma) \leq \eta\right\}$. Since $V(\rho, \gamma)$ is radially unbounded, the set $\mathcal{S}_\eta$ is compact and its boundary is given by $\partial\mathcal{S}_\eta = \left\{(\rho, \gamma) : \left(V(\rho, \gamma) = \eta \ \wedge\ \gamma < \frac{3}{2}\pi\right) \ \vee\ \left(V(\rho, \gamma) \leq \eta \ \wedge\ \gamma = \frac{3}{2}\pi\right)\right\}$. We want to show that the set $\mathcal{S}_\eta$ is a *viability domain* for the system (20), i.e. the vector field always belongs to the *contingent cone* to $\mathcal{S}_\eta$, at any point on $\partial\mathcal{S}_\eta$ (see Figure 3, and (Aubin, 1991, p. 25-26) for a rigorous definition).
Consider $(\rho, \gamma) \in \partial\mathcal{S}_\eta$ such that $\gamma < \frac{3}{2}\pi$, $V(\rho, \gamma) = \eta$. Since for such (ρ, γ) the function V is differentiable and $\dot{V}(\rho, \gamma) \leq 0$, it can be concluded that the vector field belongs to the contingent cone to $\mathcal{S}_\eta$ (see e.g. point P_1 in Figure 3) .
Consider now, if there exists, any $(\rho, \gamma) \in \partial\mathcal{S}_\eta$ such that $\gamma = \frac{3}{2}\pi$, $V(\rho, \gamma) < \eta$. Because of (13), the vector field in the r.h.s. of (20) is $[0 \ \ -\alpha]'$, with $\alpha > 0$. Hence, it belongs to the contingent cone (Figure 3, point P_2).
Finally consider, if there exists, any $(\rho, \gamma) \in \partial\mathcal{S}_\eta$ such that $\gamma = \frac{3}{2}\pi$, $V(\rho, \gamma) = \eta$. Notice that for such (ρ, γ), one has $\nabla V(\rho, \gamma) = [A(\rho), B(\frac{3}{2}\pi)] = [\beta\ 0]$, with $\beta \in \mathbb{R}$. Hence, one of the two edges of the contingent cone to $\partial\mathcal{S}_\eta$ is orthogonal to the line $\gamma = \frac{3}{2}\pi$ (Figure 3, point P_3). Again, one has that the r.h.s. of (20) is of the form $[0 \ \ -\alpha]'$, $\alpha > 0$, and hence it is tangent to the contingent cone.
Now, notice that the vector field (20) is Lipschitz on $\mathcal{S}_\eta$. Hence, by applying the Nagumo theorem (Aubin, 1991, Theorem 1.2.4, p. 28), for any $(\rho(0), \gamma(0)) \in \mathcal{S}_\eta$ the unique solution of (20) will not leave $\mathcal{S}_\eta$ for any $t \geq 0$. In other words, $\mathcal{S}_\eta$ is a *positively invariant set* with respect to system (20).

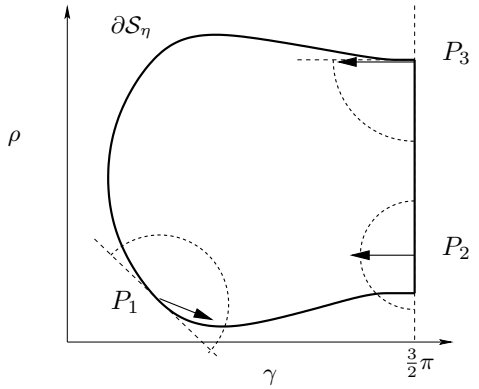

Fig. 3. Examples of contingent cones for different points on $\partial\mathcal{S}_\eta$ (dashed). Arrows represent the vector field (20).

By recalling that $\dot{V}(\rho, \gamma) \leq 0, \forall(\rho, \gamma) \in \bar{\mathcal{D}}$, one can apply LaSalle's Invariance Principle (see e.g. (Khalil, 1992)) to conclude that the trajectories starting in $\mathcal{S}_\eta$ converge asymptotically to the largest invariant set $\mathcal{M}$ such that $\mathcal{M} \subseteq E = \{(\rho, \gamma) \in \mathcal{S}_\eta : \dot{V}(\rho, \gamma) = 0\}$. It is trivial to show that, for any $\eta \geq 0$, the set $\mathcal{M}$ contains only the equilibrium point p_e. Being the initial choice of $(\rho(0), \gamma(0)) \in \bar{\mathcal{D}}$ arbitrary, convergence to p_e occurs for any trajectory starting in $\bar{\mathcal{D}}$. Because the equilibrium point p_e corresponds to counterclockwise circular motion around the beacon $\mathbf{r}_b$ with radius ρ_e, it can be concluded that such motion is a globally asymptotically stable limit cycle for the system (1)-(6). □

Remark 1 The stability analysis of this section holds for a larger class of functions $g(\rho)$, than the one proposed in (5). Let $g(\rho)$ be any locally Lipschitz function such that $|g(0)| < \infty$, (13) holds and $A(\rho)$ in (16) satisfies: (i) $\exists!\ \rho_e$ s.t. $A(\rho_e) = 0$; (ii) $\lim_{\rho\to+\infty} \int_{\rho_e}^{\rho} A(\sigma)d\sigma = +\infty$; (iii) $\lim_{\rho\to 0^+} \int_{\rho_e}^{\rho} A(\sigma)d\sigma = +\infty$. Then, the counterclockwise circular motion of radius ρ_e is globally asymptotically stable for system (1)-(6). Hence, global stability is guaranteed, for example, by any $g(\rho)$ constant and positive. The choice of the form (5) is motivated by an additional degree of freedom for tuning the control law in the multi-vehicle case (see Section 4.3).
It is worth remarking that in order to stabilize the clockwise rotation, it suffices to choose the threshold $\psi \in (0, \frac{\pi}{2})$. In this case, constraint (13) guarantees that the clockwise rotation is the only limit cycle.

3 Multi-vehicle systems

In this section the control law (4) is modified in order to deal with a multi-vehicle scenario. Consider a group of n agents whose motion is described by equations

$$\dot{x}_i(t) = v\, \cos\theta_i(t) \tag{21}$$
$$\dot{y}_i(t) = v\, \sin\theta_i(t) \tag{22}$$
$$\dot{\theta}_i(t) = u_i(t), \tag{23}$$

with $i = 1 \dots n$. Let ρ_i and γ_i be defined as in Section 2; ρ_{ij} and γ_{ij} denote respectively the linear and angular distance between vehicle i and vehicle j (see Figure 4). In the control input $u_i(t)$ a new additive term is introduced which depends on the interaction between the i-th vehicle and any other perceived vehicle j

$$u_i(t) = f_{ib}(\rho_i, \gamma_i) + \sum_{j \in \mathcal{N}_i(t)} f_{ij}(\rho_{ij}, \gamma_{ij}). \qquad (24)$$

In (24), f_{ib} is the same as in the r.h.s. of (4), i.e.

$$f_{ib}(\rho_i, \gamma_i) = \begin{cases} k_b \cdot g(\rho_i; c_b, \rho_0) \cdot \alpha_d(\gamma_i) & \text{if } \rho_i > 0 \\ 0 & \text{if } \rho_i = 0, \end{cases} \qquad (25)$$

while

$$f_{ij}(\rho_{ij}, \gamma_{ij}) = k_v \cdot g(\rho_{ij}; c_v, d_0) \cdot \beta_d(\gamma_{ij}), \qquad (26)$$

where $k_v > 0$, $c_v > 1$, $d_0 > 0$ and

$$\beta_d(\gamma_{ij}) = \begin{cases} \gamma_{ij} & \text{if } 0 \le \gamma_{ij} \le \pi \\ \gamma_{ij} - 2\pi & \text{if } \pi < \gamma_{ij} < 2\pi. \end{cases} \qquad (27)$$

The set $\mathcal{N}_i(t)$ contains the indexes of the vehicles that at time t lie inside the *visibility region* $\mathcal{V}_i$, that is the region where it is assumed that the sensors of the i-th vehicle can perceive other vehicles. Notice that the sets $\mathcal{N}_i(t)$ are time-varying, which implies that the control law (24) switches every time a vehicle enters into or exits from the region $\mathcal{V}_i$. To simplify the notation, the dependence on t of $\mathcal{N}_i(t)$ is dropped hereafter.

In this paper, the visibility region has been chosen as the union of two sets (see Figure 5): (i) a circular sector of radius d_l and angular amplitude $2\alpha_v$ centered at the vehicle, modeling the presence of a long range sensor with limited angular visibility (e.g., a laser range finder); (ii) a circular region around the vehicle of radius d_s, which models a proximity sensor (e.g., a ring of sonars) and plays the role of a "safety region" around the vehicle. Therefore, one has that $j \in \mathcal{N}_i$ if and only if one of the following conditions is verified: (i) $|\rho_{ij}| \le d_l$ and $|\beta_d(\gamma_{ij})| \le \alpha_v$; (ii) $|\rho_{ij}| \le d_s$. The design parameter d_0 is the desired distance between two consecutive vehicles rotating around the beacon. Hereafter, it is obviously assumed that $d_s < d_0 < d_l$ and $d_0 < 2\rho_e$. Moreover, the parameters ρ_e and d_0 will be chosen so that each vehicle can perceive another vehicle when rotating around the beacon, i.e. $\arcsin\left(\frac{d_0}{2\rho_e}\right) < \alpha_v$.

The motivation for the control law (24)-(27) relies in the fact that each agent i is driven by the term $f_{ib}(\cdot)$ towards the counterclockwise circular motion about the beacon, while the terms $f_{ij}(\cdot)$ have a twofold aim: to enforce $\rho_{ij} = d_0$ for all the agents $j \in \mathcal{N}_i$ and, at the same time, to favor collision-free trajectories. Indeed, the i-th vehicle is attracted by any vehicle $j \in \mathcal{N}_i$ if $\rho_{ij} > d_0$, and repulsed if $\rho_{ij} < d_0$. Moreover, the term $g(\rho_{ij}; c_v, d_0)$ in

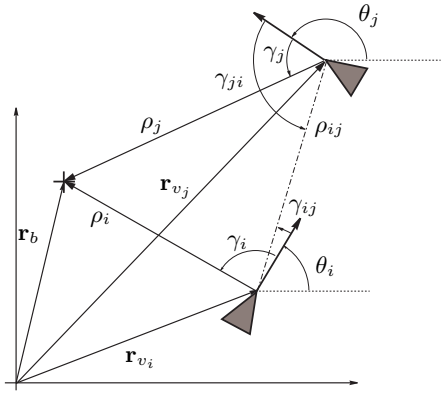

Fig. 4. Two vehicles (triangles) and a beacon (cross).

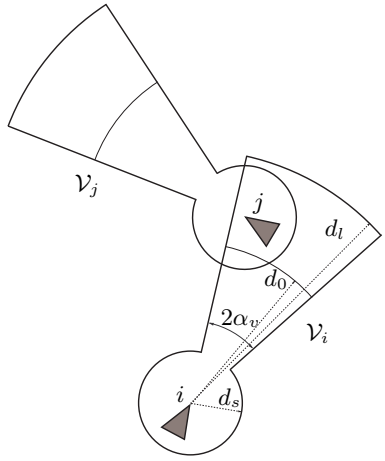

Fig. 5. Visibility region of i-th and j-th vehicle.

(26) is always negative for $\rho_{ij} < d_s$, thus pushing the j-th agent outside the circular safety region around the i-th vehicle and therefore hindering collisions among the vehicles. The expected result of such combined actions is that the agents safely reach the counterclockwise circular motion in a number of platoons, in which the distances between consecutive vehicles is d_0. In the following, local stability analysis of system (21)-(23) under the control law (24)-(27), is addressed.

3.1 Equilibrium configurations

From Section 2 and by using a coordinate transformation similar to the one adopted in (Marshall *et al.*, 2004), one obtains the equations

$$\dot{\rho}_i = -v \cos\gamma_i \qquad (28)$$

$$\dot{\gamma}_i = \frac{v}{\rho_i} \sin\gamma_i - u_i \qquad (29)$$

$$\dot{\rho}_{ij} = -v\,(\cos\gamma_{ij} + \cos\gamma_{ji}) \qquad (30)$$

$$\dot{\gamma}_{ij} = \frac{v}{\rho_{ij}}\,(\sin\gamma_{ij} + \sin\gamma_{ji}) - u_i \qquad (31)$$

$\forall i, j = 1 \dots n, j \neq i$. Notice that there are algebraic relationships among the state variables $\rho_i, \gamma_i, \rho_{ij}, \gamma_{ij}$, which

will be taken into account in the stability analysis. The following result provides equilibrium configurations for the considered multi-vehicle system.

Proposition 2 *Every configuration of n vehicles in counterclockwise circular motion about a fixed beacon, with rotational radius $\rho_i = \rho_e$ defined in* (14)*, and*

$$\rho_{ij} = d_0 \qquad \forall i = 1 \dots n, \ \textit{and} \ \forall j \in \mathcal{N}_i, \tag{32}$$

corresponds to an equilibrium point of system (28)-(31)*, under the control law* (24)-(27)*.*

Proof: The counterclockwise circular motion implies $\gamma_i = \frac{\pi}{2}$, and hence $\dot{\rho}_i = 0$. Now, notice that $\rho_{ij} = d_0$ for any $j \in \mathcal{N}_i$ implies that $f_{ij}(\cdot) = 0$. Hence u_i in (24) is equal to (4). From (14), $\rho_i = \rho_e$ implies $\dot{\gamma}_i = 0$. Since all the vehicles lie on the same circle of radius ρ_e, with the same direction of rotation, by trivial geometric considerations it can be shown that $\gamma_{ij} + \gamma_{ji} = \pi$ and $\min\{\gamma_{ij}, \gamma_{ji}\} = \arcsin\left(\frac{\rho_{ij}}{2\rho_e}\right)$. Hence $\dot{\rho}_{ij} = 0$ due to (30). Moreover, by exploiting (14) again, equation (31) becomes $\dot{\gamma}_{ij} = 2\,\frac{v}{\rho_{ij}}\,\sin\gamma_{ij} - \frac{v}{\rho_e} = 0$, which concludes the proof. □

A necessary condition for the existence of equilibrium configurations satisfying (32) is that d_0 and ρ_e are chosen so that

$$(n-1)\,\arcsin\left(\frac{d_0}{2\rho_e}\right) + \varphi < \pi. \tag{33}$$

where

$$\varphi = \min\left\{\alpha_v\,,\ \arcsin\Big(\frac{d_l}{2\rho_e}\Big)\right\} \tag{34}$$

(with a slight abuse of notation, it is meant that $\varphi = \alpha_v$ whenever $d_l > 2\rho_e$). This choice guarantees that the n vehicles can lie on a circle of radius ρ_e, with distance d_0 between two consecutive vehicles and with at least one vehicle that does not perceive any other vehicle. In (33), φ represents the maximum angular distance γ_{ij} such that the i-th vehicle perceives the j-th one, when the two vehicles are moving in circular motion with rotational radius ρ_e (see Figure 6).

Let us consider visibility regions $\mathcal{V}_i$ with $\alpha_v \leq \pi/2$ (typical e.g. for range finders). Condition (32) in Proposition 2 requires that a vehicle in circular motion with radius ρ_e perceives at most one vehicle, i.e. $\mathrm{card}(\mathcal{N}_i) \in \{0, 1\}$. A sufficient condition for (32) to hold is, e.g., that d_0 and ρ_e satisfy

$$2\arcsin\left(\frac{d_0}{2\rho_e}\right) > \varphi, \tag{35}$$

with φ given by (34), so that in the equilibrium configuration, a vehicle cannot perceive two vehicles within its visibility region. Notice that condition (35) also guarantees that there is a neighborhood of the equilibrium configuration in which the sets $\mathcal{N}_i$ (and hence the interconnection topology) do not change.

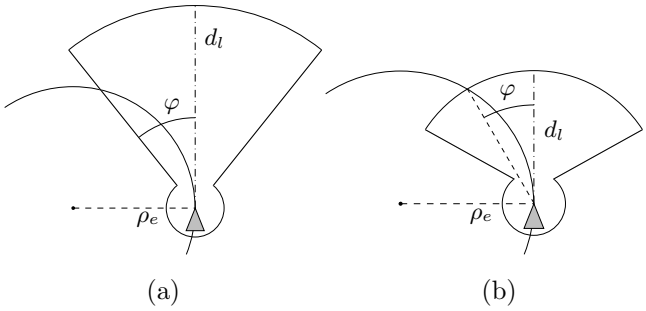

Fig. 6. Possible values of φ in constraint (33): (a) $\varphi = \alpha_v$; (b) $\varphi = \arcsin\Big(\frac{d_l}{2\rho_e}\Big)$.

When (33) and (35) are satisfied, there can be several different equilibrium configurations such as those considered in Proposition 2. Indeed, due to (33) all vehicles can lie on the desired circle of radius ρ_e and there is at least one vehicle that does not perceive the others, while (35) guarantees that *at the equilibrium* $\mathrm{card}(\mathcal{N}_i) \in \{0, 1\}$. This means that there may be q vehicles with $\mathrm{card}(\mathcal{N}_i) = 0$ and $n - q$ vehicles with $\mathrm{card}(\mathcal{N}_i) = 1$, i.e. the equilibrium configuration is made of q separate platoons. The limit cases are obviously $q = 1$ (a unique platoon) and $q = n$ (n vehicles rotating independently around the beacon).

Remark 2 It is worth discussing the relationships between the proposed approach and the techniques that aim at equilibrium formations in cyclic pursuit (see e.g. (Marshall *et al.*, 2004)). Although the objective is basically the same (to achieve collective circular motion), the main difference is that the present approach does not enforce a fixed interconnection topology among the vehicles. The only requirement is that there exist some of the equilibrium configurations considered in Proposition 2. Notice that this can be always guaranteed by acting on the control law parameters so that conditions (33) and (35) are satisfied (see the discussion in Section 4.3). The advantage of this approach is that there is no need to number the agents and to make them distinguishable. In turn, one must be prepared to accept that the vehicles achieve the circular motion in different configurations, possibly made up of separate platoons, while the cyclic-pursuit approach requires a unique platoon with no distinct leader and a fixed interconnection topology.

3.2 Stability analysis

Let us now proceed with stability analysis of the multi-vehicle system (28)-(31), with the control law (24)-(27), under the assumptions (13), (33) and (35). In particular, the aim is to establish sufficient conditions under which the equilibrium configurations in Proposition 2 are asymptotically stable.

W.l.o.g., consider n vehicles in counterclockwise circular motion about a beacon, forming a single platoon and numbered as in Figure 7 (the analysis of equilibria with

multiple platoons is analogous). The equilibrium point considered by Proposition 2 is such that

$$\begin{aligned} &\rho_i = \rho_e \qquad \gamma_i = \tfrac{\pi}{2} \qquad\quad i = 1 \dots n \\ &\gamma_{(i-1)i} = \tfrac{\pi}{2} + \arccos(\tfrac{d_0}{2\rho_e}) \;\; i = 2 \dots n. \end{aligned} \tag{36}$$

Being $\text{card}(\mathcal{N}_1) = 0$ and $\text{card}(\mathcal{N}_i) = 1$ for $i \geq 2$, the kinematic of the i-th vehicle is locally affected only by the positions of the beacon and of the $(i-1)$-th vehicle, except for vehicle 1 whose kinematic is locally determined only by the beacon position. Therefore, in a neighborhood of the equilibrium configuration (36), the kinematic system (28)-(31) is described by the equations

$$\dot{\rho}_1 = -v \cos\gamma_1 \tag{37}$$

$$\dot{\gamma}_1 = \frac{v}{\rho_1} \sin\gamma_1 - u_1 \tag{38}$$

$$\dot{\rho}_i = -v \cos\gamma_i \tag{39}$$

$$\dot{\gamma}_i = \frac{v}{\rho_i} \sin\gamma_i - u_i \tag{40}$$

$$\dot{\gamma}_{(i-1)i} = \frac{v}{\rho_{(i-1)i}} (\sin\gamma_{(i-1)i} + \sin\gamma_{i(i-1)}) - u_{i-1} \tag{41}$$

for $i = 2 \dots n$. The control inputs are given by $u_1 = f_{1b}$ and $u_i = f_{ib} + f_{i(i-1)}$ for $i \geq 2$. Notice that the $3n-1$ state variables in system (37)-(41) are sufficient to describe completely the n-vehicles system. Indeed, the remaining state variables in system (28)-(31) can be obtained via algebraic relationships form the above $3n-1$ ones. In particular one has

$$\begin{aligned} \rho_{(i-1)i} = &\rho_{(i-1)} \cos(\gamma_{(i-1)i} - \gamma_{(i-1)}) + \\ &+\sqrt{\rho_i^2 - \rho_{(i-1)}^2 \sin^2(\gamma_{(i-1)i} - \gamma_{(i-1)})} \end{aligned} \tag{42}$$

$$\gamma_{i(i-1)} = \gamma_i - \arcsin\left(\frac{\rho_{(i-1)}}{\rho_i} \sin(\gamma_{(i-1)i} - \gamma_{(i-1)})\right) \tag{43}$$

for $i = 2, \dots, n$.
By linearizing system (37)-(41) at the equilibrium point (36), one gets a system of the form

$$\dot{\xi} = \begin{bmatrix} A & 0 & \cdots & 0 \\ * & B & \ddots & \vdots \\ \vdots & \ddots & \ddots & 0 \\ * & \cdots & * & B \end{bmatrix} \xi \tag{44}$$

where $\xi = [\rho_1 \; \gamma_1 \; \rho_2 \; \gamma_2 \; \gamma_{12} \; \dots \; \rho_n \; \gamma_n \; \gamma_{(n-1)n}]'$, $A \in \mathbb{R}^{2\times 2}$ and $B \in \mathbb{R}^{3\times 3}$. The next lemma is instrumental in establishing a sufficient condition for asymptotic stability of the considered equilibrium configurations.

Lemma 3 *If the parameters of the control law* (24)-(27) *satisfy*

$$\frac{k_v}{k_b} \leq 2 \frac{c_v}{c_b} \frac{c_b - 1}{c_v - 1} \tag{45}$$

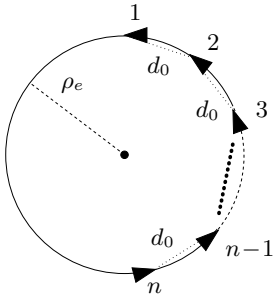

Fig. 7. Equilibrium configuration of n vehicles: $\mathcal{N}_i = \{i-1\}$ and $\rho_{i(i-1)} = d_0$ for $i = 2, \dots, n$, while $\mathcal{N}_1$ is empty.

then matrix B in (44) *is Hurwitz.*

Proof: See Appendix C. □
Now, the main result of this section can be stated.

Theorem 2 *Let* (45) *hold. Then, every equilibrium configuration given by Proposition 2 is asymptotically stable.*

Proof: It is sufficient to show that the lower triangular matrix in (44) is Hurwitz. According to Lemma 3, the inequality (45) guarantees that matrix B is Hurwitz. Then, it remains to show that also matrix A in (44) is Hurwitz. From the linearization of (37)-(38) at the equilibrium point (36), one gets $A = \begin{bmatrix} 0 & a_{12} \\ a_{21} & a_{22} \end{bmatrix}$ where $a_{12} = v$, $a_{21} = -\frac{v}{\rho_e^2} - k_b \frac{c_b - 1}{(c_b-1)\rho_e + \rho_0} \frac{\pi}{2}$, $a_{22} = -\frac{2v}{\pi \rho_e}$. Being $a_{12} > 0$, $a_{21} < 0$ and $a_{22} < 0$, matrix A is Hurwitz. This concludes the proof. □
Clearly (45) is a sufficient conditions and its violation does not imply instability of the considered equilibria. However, it is worth noticing that a wrong choice of the control law parameters may lead to an unstable matrix B in (44), and hence to instability of the equilibrium configuration: examples can be easily found for $c_v = c_b$ and $k_v \gg k_b$, or for $k_v = k_b$ and $c_v \gg c_b$. This is in good agreement with intuition, as it basically says that the beacon-driven control term should not be excessively reduced with respect to the control input due to interaction with the other agents.

4 Simulation results

In this section, simulation studies are provided for the multi-vehicle system (21)-(23) under the control law (24)-(27). In the examples, the velocity of the vehicles is set to $v = 1$ and the visibility region $\mathcal{V}_i$ has been chosen as in Figure 5, with $\alpha_v = \frac{\pi}{4}$, $d_s = 3$, $d_l = 12$. The control law parameters are set to: $\psi = \frac{7}{4}\pi$, $d_0 = 10$, $c_b = c_v = 2$, $k_b = 0.05$, $k_v = 0.09$ (notice that condition (45) is satisfied). Throughout the simulations, the parameter ρ_0 is used as a tuning knob to properly adjust the rotational radius ρ_e resulting from (14) and to enforce the constraints (13), (33) and (35) (see Section 4.3 below for a detailed discussion).

4.1 *Static beacon*

A 8-vehicle system with $\rho_0 = 12$ is considered. A typical simulation run is shown in Figure 8(a). The multi-vehicle system achieves collective circular motion in three separate platoons of cardinality 4, 3 and 1 respectively (i.e., $q = 3$ according to the discussion in Section 3.1). In Figures 8(b)-8(c), the evolution of the average rotational radius $\bar{\rho} = \frac{1}{n}\sum_{i=1}^{n} \rho_i$ and of the average angular distance with respect to the beacon $\bar{\gamma} = \frac{1}{n}\sum_{i=1}^{n} \gamma_i$ are plotted.
Figure 9 shows four consecutive snapshots of a simulation in which an initial equilibrium configuration of five vehicles, rotating around the beacon in two platoons, is perturbed by a sixth incoming vehicle. It can be observed that, after a transient in which the original equilibrium is destroyed due to the interaction between vehicles 5 and 6, the agents reorganize themselves to finally reach a new equilibrium consisting of one single platoon. Observe that the final interconnection topology is different from that of the initial equilibrium.
Repeated runs have been performed to test convergence of the multi-vehicle system, for different initial configurations. In Figure 10(a), the estimated convergence times for 100 simulations with random initial conditions are reported, for a 4-vehicle system with $\rho_0 = 5$. The same is done in Figure 10(b), for a 6-vehicle system with $\rho_0 = 8$. The convergence test is based on the difference between the rotational radius of each vehicle and ρ_e (namely $|\rho_i(t) - \rho_e|$). All the simulations terminated successfully in both cases. Quite intuitively, one observes that the average convergence time increases as the number of vehicles grows.

4.2 *Moving beacon*

Although the theoretical analysis has been performed for the case of a static beacon, the proposed control strategy is expected to show good performance also when the beacon is moving and the team of vehicles has to track it, while keeping collective circular motion around it. Moreover, the control law has been designed so that when the beacon moves faster than the vehicles, or it is faraway from them, each vehicle points straight towards the beacon and tracks it in rectilinear motion. In fact, when ρ is large, from (12) one has that γ tends to 0 (or to 2π, if it starts from values larger than ψ), and hence $\dot{\rho}$ tends to be equal to $-v$, as desired.
In Figure 11, the beacon moves in rectilinear motion (dashed line) with constant velocity $v_b = 0.1$, while a 4-vehicle team is subject to the usual control law with $v = 1$ and $\rho_0 = 5$. Notice that the team tracks the beacon while maintaining a circular motion around it. In Figure 12, a 6-vehicle team has to deal with a non-static beacon, which jumps through four sequential way-points $\mathbf{r}_{b_i}$, $i = 1, \ldots, 4$ (a similar scenario was considered in (Paley *et al.*, 2004)). It can be observed that when the beacon switches from $\mathbf{r}_{b_i}$ to $\mathbf{r}_{b_{i+1}}$, the vehicles move from a rotational configuration about $\mathbf{r}_{b_i}$ towards the new beacon position $\mathbf{r}_{b_{i+1}}$, in a sort of parallel motion (see Figure 12). Notice that this is obtained without switching between two different control laws (as done in (Paley *et al.*, 2004)). The trajectories show that the desired con-

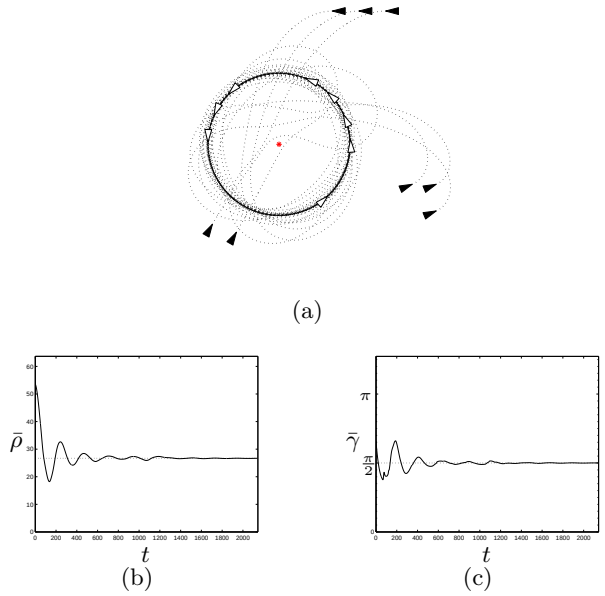

Fig. 8. A 8-vehicle scenario: (a) trajectory of 8 vehicles; (b) average rotational radius; (c) average angular distance .

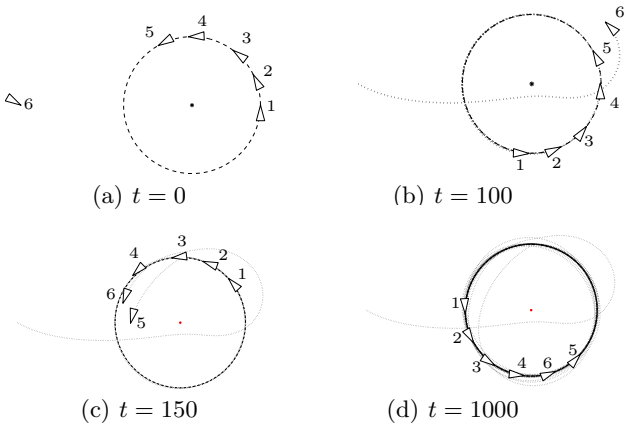

Fig. 9. Team self reorganizing after the incoming of a new vehicle.

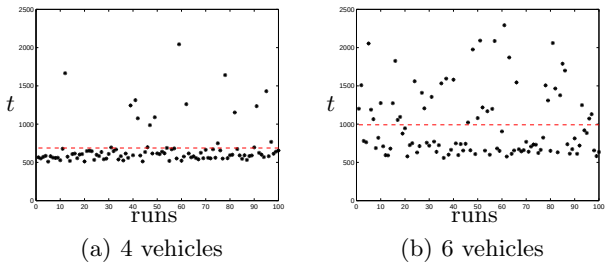

Fig. 10. Convergence times for 100 runs; the dotted line represents the average convergence time.

figuration in rotational motion is reached for each waypoint.

4.3 Design of the control law parameters

The transient behavior of the multi-vehicle system is clearly affected by the choice of the control law parameters. Following the discussion in Section 3.1 the role of the constraints (13),(33) and (35) is analyzed next.
The clockwise rotation around the beacon must not be an equilibrium point, i.e. the parameters have to verify inequality (13). This can be obtained by choosing a sufficiently small ρ_0, or alternatively a sufficiently small control gain k_b in (25). The equilibrium radius ρ_e must be consistent with the number of vehicles and the desired inter-vehicle distance d_0. This means that the configuration of a single platoon in circular motion must be feasible with respect to inequality (33). Notice that this requires a sufficiently large ρ_e (for fixed d_0), and therefore a sufficiently large ρ_0. This introduces a trade-off with the requirement imposed by (13). On the other hand, since ρ_e can be increased by suitably reducing k_b, it is always possible to find a sufficiently small k_b satisfying both (13) and (33). However, a too small k_b may lead to violation of the sufficient condition (45), and hence stability of the desired circular collective motion is not guaranteed anymore.
Figure 13 shows the region of feasible parameters k_b and ρ_0, for the simulation examples presented in this section. The region below the dashed curve contains the values of k_b and ρ_0 satisfying (13). Constraint (33) is satisfied by all the pairs (k_b, ρ_0) above the solid line corresponding to the number of vehicles n (Figure 13 reports the cases $n = 4, 6, 8$). The constraint (35) turns out to be always satisfied in the considered example. Finally, the sufficient condition (45) of Theorem 2 is satisfied by all values of k_b lying on the right of the dash-dotted line (notice that for $c_b = c_v$, condition (45) simplifies to $k_b \geq \frac{k_v}{2}$). Therefore, by choosing k_b and ρ_0 inside the region bounded by the three curves described above (the one corresponding to $n = 8$ is shaded in Figure 13), it is possible to satisfy all the geometrical constraints and the stability condition. It can be checked that this has been done in all the examples presented in this section.
So far, it has been assumed that the parameter k_v is assigned. However, the choice of k_v is driven by a trade-off between safety and stability. Indeed, notice that the multi-vehicle system with $k_v = 0$ is globally asymptotically stable, because it is the composition of globally asymptotically stable decoupled subsystems. Instability can arise only from the presence of the cross terms f_{ij} in (26). In this respect, the choice of a small k_v is motivated by the stability constraint (45), while a large k_v favors safe trajectories (as it increases repulsion between nearby vehicles) and a tighter connection among the vehicles in the team (because attraction is stronger between faraway vehicles).
Several simulations have been performed in order to analyze the behavior of the multi-vehicle system for different values of k_v. Figure 14 refers to a 4-vehicle setting with $\rho_0 = 5$. It shows the convergence times (Fig. 14(a))

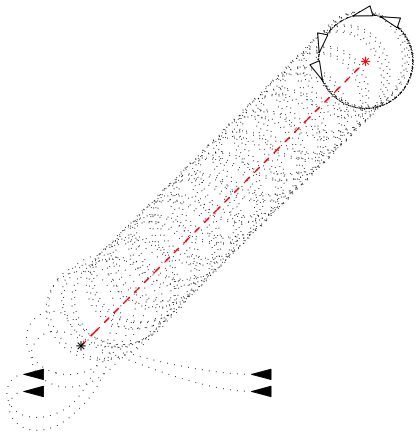

Fig. 11. A 4-vehicle team tracking a moving beacon.

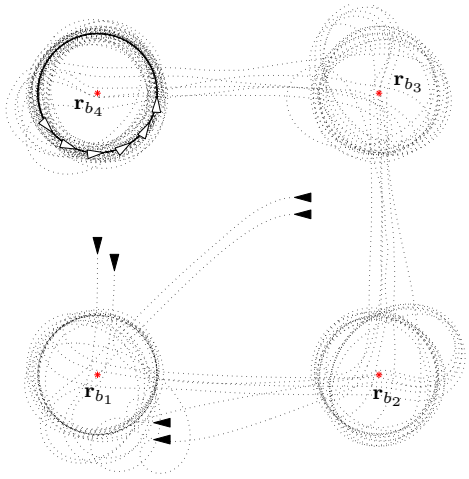

Fig. 12. A 6-vehicle team tracking four sequential way points.

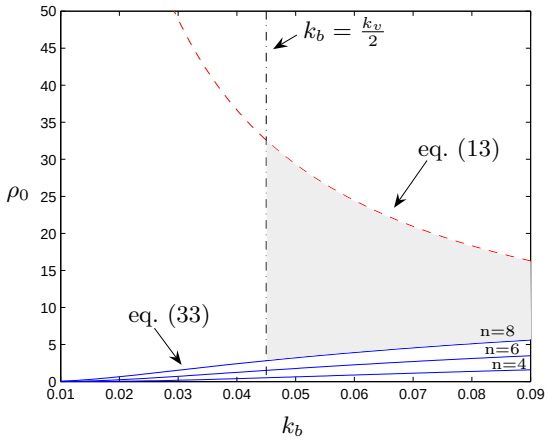

Fig. 13. Feasible region for parameters k_b and ρ_0

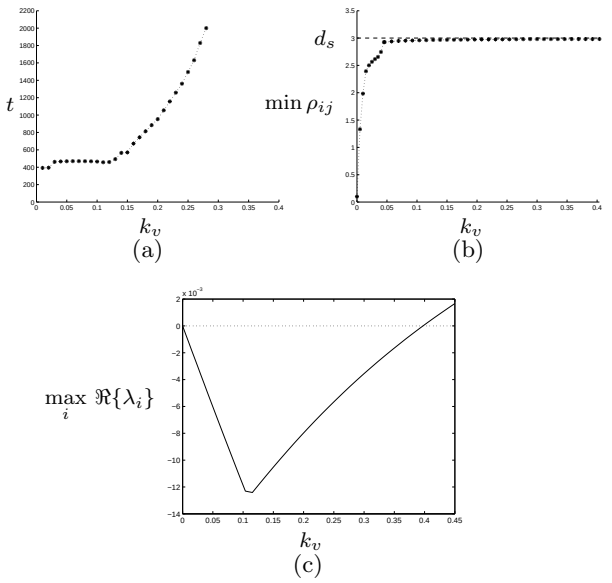

Fig. 14. Simulations of a 4-vehicle system for different values of k_v: (a) convergence times; (b) minimum inter-vehicle distance; (c) maximum real part of the eigenvalues of matrix B.

and the minimum distance between two vehicles in the team, $\min_{i,j} \min_t \rho_{ij}(t)$ (Fig. 14(b)), both as functions of k_v. Although the sufficient condition (45) is satisfied for $k_v \leq 0.1$, by computing the eigenvalues of matrix B it turns out that, for the set of parameters considered in this simulations, instability is reached only for $k_v \geq 0.4$ (Fig. 14(c)). This effect is clearly depicted in Figure 14(a) where the convergence time rapidly grows as k_v approaches the instability threshold. On the other hand, the minimum inter-vehicle distance, which is representative of the collision avoidance effect, does not change significantly for $k_v > 0.1$, while it is remarkably reduced for smaller values of k_v. This shows the presence of a trade-off between convergence time and safety requirements. Notice also that for values of k_v larger than 0.05 the minimum inter-vehicle distance is approximately equal to the radius d_s of the safety circular area in the visibility region $\mathcal{V}_i$. This confirms that the cross-term f_{ij} in the control law (24) tends to keep the vehicle j outside the safety region of the i-th agent, thus enforcing safe trajectories in presence of finite size vehicles.

5 Conclusions and future work

In this paper, a decentralized control law for a team of nonholonomic vehicles, whose aim is to achieve collective circular motion around a virtual reference beacon, has been presented. The main features of the proposed control strategy are: i) it guarantees global stability in the single-vehicle case; ii) control parameters can be easily selected to achieve local stability of the equilibrium configurations in the multi-vehicle scenario; iii) simulative studies show promising results in terms of convergence rate and tracking performance, in the case of a non-static beacon. With respect to similar approaches presented in the literature, quite restrictive assumptions have been removed. In particular: (i) limitations in the visibility region $\mathcal{V}_i$ of the vehicles are explicitly taken into account; (ii) exteroceptive orientation measurements are not performed: each vehicle has to measure only distances to other vehicles lying in its visibility region; (iii) labelling of the vehicles is not required. These aspects are critical for multi-vehicle systems with equipment limitations, hampering long range measurements or estimation of other vehicles orientation. Moreover, there is no need of smart communication protocols to identify vehicles or to exchange information, because the required measurements can be obtained from range sensors.

Several interesting developments of this work can be foreseen. From a theoretical point of view, it would be desirable to provide sufficient conditions for the convergence of the multi-vehicle system to the desired equilibrium configurations. Simulation studies seem to suggest that collective circular motion is always achieved, whenever the initial configuration of the multi-vehicle system is chosen at random. Another research line to be pursued concerns the use of the proposed control law for tracking a moving beacon, while keeping collective circular motion around it. As it has been observed, the control law has been designed so that, when the beacon is faraway from the vehicles, each agent points straight towards it. Hence, smooth transitions between circular and parallel motion are expected when tracking a beacon with time-varying velocity profile. Rigorous theoretical analysis and extensive performance evaluations are necessary to validate the proposed control scheme in the tracking scenario.

References

Aubin, J. P. (1991). *Viability theory*. Birkhauser.

Ceccarelli, N., M. Di Marco, A. Garulli and A. Giannitrapani (2005). Collective circular motion of multi-vehicle systems with sensory limitations. In: *Proc. of the IEEE Conference on Decision and Control*. Seville. pp. 740–745.

Ferrari-Trecate, G., A. Buffa and M. Gati (2006). Analysis of coordination in multi-agent systems through partial difference equations. *IEEE Trans. on Automatic Control* **51**(6), 1058–1063.

Jadbabaie, A., J. Lin and A. S. Morse (2003). Coordination of groups of mobile autonomous agents using nearest neighbor rules. *IEEE Trans. on Automatic Control* **48**(6), 988–1001.

Jeanne, J., N. E. Leonard and D. Paley (2005). Collective motion of ring-coupled planar particles. In: *Proc. of the IEEE Conference on Decision and Control*. Seville. pp. 3929–3934.

Justh, E. W. and P. S. Krishnaprasad (2004). Equilibria and steering laws for planar formations. *Systems and Control Letters* **52**, 25–38.

Khalil, H. (1992). *Nonlinear Systems*. New York: Macmillan Publishing Co.

Leonard, N. E. and E. Fiorelli (2001). Virtual leaders, artificial potentials and coordinated control of groups. In: *Proc. of the IEEE Conference on Decision and Control*. Orlando. pp. 2968–2973.

Lin, Z., M. E. Broucke and B. A. Francis (2004). Local control strategies for groups of mobile autonomous agents. *IEEE Trans. on Automatic Control* **49**(4), 622–629.

Marshall, J. A., M. E. Broucke and B. A. Francis (2004). Formations of vehicles in cyclic pursuit. *IEEE Trans. on Automatic Control* **49**(11), 1963–1974.

Moreau, L. (2005). Stability of multiagent systems with time-dependent communication links. *IEEE Trans. on Automatic Control* **50**(2), 169–182.

Olfati-Saber, R. and R. M. Murray (2004). Consensus problems in networks of agents with switching topology and time-delays. *IEEE Trans. on Automatic Control* **49**(9), 1520–1533.

Paley, D., N. E. Leonard and R. Sepulchre (2004). Collective motion: bistability and trajectory tracking. In: *Proc. of the IEEE Conference on Decision and Control*. Nassau, Bahamas. pp. 1932–1936.

Reynolds, C. (1987). Flocks, birds, and schools: a distributed behavioral model. *Computer Graphics* **21**, 25–34.

Sepulchre, R., D.A. Paley and N.E. Leonard (2007). Stabilization of planar collective motion: All-to-all communication. *IEEE Trans. on Automatic Control* **52**(5), 811–824.

Tanner, HG, A. Jadbabaie and GJ Pappas (2007). Flocking in fixed and switching networks. *IEEE Trans. on Automatic Control* **52**(5), 863–868.

Vicsek, T., A. Czirok, E. B. Jacob, I. Cohen and O. Schochet (1995). Novel type of phase transitions in a system of self-driven particles. *Physical Review Letters* **75**, 1226–1229.

Xiao, L. and S. Boyd (2004). Fast linear iterations for distributed averaging. *System and Control Letters* **53**(1), 65–78.

A Proof of Lemma 1

Let $\hat{\mathcal{D}}_1 = \mathbb{R}_{++} \times (\frac{3}{2}\pi, \beta]$, $\hat{\mathcal{D}}_2 = \mathbb{R}_{++} \times (\beta, 2\pi)$, where β is such that $\dot{\gamma} < -\xi < 0$ for any $(\rho, \gamma) \in \hat{\mathcal{D}}_1$, for some $\xi > 0$. Notice that such β can always be found because of (13). Observe that for any $(\rho, \gamma) \in \hat{\mathcal{D}}$, one has $\dot{\rho} < 0$ but, despite the discontinuity in (12), also $\lim_{\rho \to 0^+} \dot{\gamma}(\rho, \gamma) = -\infty$, $\forall \gamma \in (\frac{3}{2}\pi, 2\pi)$, and hence the trajectories cannot reach $\rho = 0$ within $\hat{\mathcal{D}}$ in finite time. Moreover, because $V(\rho, \gamma)$ is radially unbounded on $\mathcal{D}$ and $\dot{V}(\rho, \gamma) < 0$ on the set $\mathcal{K}$ in (18), then the trajectories cannot leave the set $\hat{\mathcal{D}}$ through the line $\gamma = 2\pi$.

Now consider any initial condition $(\rho(0), \gamma(0)) \in \hat{\mathcal{D}}_2$. In such set, one has $\dot{\rho} \leq -v \cos\beta < 0$. Since there cannot exist trajectories such that $\rho(t) = 0$ or $\gamma(t) = 2\pi$ for any finite t, as shown above, one can always find a time $\bar{t}_1 \leq \frac{\rho(0)}{v \cos\beta}$ such that $\gamma(\bar{t}_1) = \beta$ and hence $(\rho(\bar{t}_1), \gamma(\bar{t}_1)) \in \hat{\mathcal{D}}_1$. Choose now any initial condition $(\rho(0), \gamma(0)) \in \hat{\mathcal{D}}_1$. Since $\dot{\gamma} < -\xi$, and there cannot exist a trajectory such that $\rho(t) = 0$ for any finite t, one can always find a time $\bar{t}_2 \leq \frac{\gamma(0) - \frac{3}{2}\pi}{\xi}$ such that $\gamma(\bar{t}_2) = \frac{3}{2}\pi$ with $\rho(\bar{t}_2) > 0$. Therefore, it has been proven that for any initial condition in $\hat{\mathcal{D}}$, there exists a finite time $\bar{t} \leq \bar{t}_1 + \bar{t}_2$ such that $(\rho(\bar{t}), \gamma(\bar{t})) \in \bar{\mathcal{D}}$.

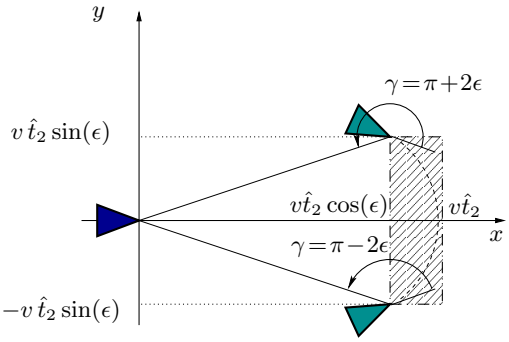

Fig. B.1. Bounds on ρ and γ at time $\hat{t}_2$.

B Proof of Lemma 2

Define the sets of initial conditions $\mathcal{B}_1 = \{(\mathbf{r}_v(0), \theta(0)) : \gamma = 0,\ 0 < \rho < \infty\}$, $\mathcal{B}_2 = \{(\mathbf{r}_v(0), \theta(0)) : \rho = 0\}$. Consider first $(\mathbf{r}_v(0), \theta(0)) \in \mathcal{B}_1$. Then, system (12) boils down to $\dot{\rho}(t) = -v$, $\dot{\gamma}(t) = 0$, $\forall t \in [0, \hat{t}_1)$ where $\hat{t}_1 = \frac{\rho(0)}{v}$. Hence the vehicle proceeds straight towards the beacon until it reaches it, i.e. $\rho(\hat{t}_1) = 0$ and hence $(\mathbf{r}_v(\hat{t}_1), \theta(\hat{t}_1)) \in \mathcal{B}_2$.

Consider now an initial condition $(\mathbf{r}_v(0), \theta(0)) \in \mathcal{B}_2$ (notice that in this case γ is not defined). We want to prove that in finite time $(\rho(t), \gamma(t)) \in \bar{\mathcal{D}}$. W.l.o.g. set $\mathbf{r}_v(0) = \mathbf{r}_b = [0, 0]'$ and $\theta(0) = 0$. Observe that system (1)-(6) does not have any equilibrium point, and that $|\dot{\theta}| < M \doteq k \log(c)\psi$ as long as $\rho \leq \rho_0$ (see (3)-(6)). Let t_0 be the smallest time t (if there exists) such that $\rho(t) = \rho_0$, otherwise set $t_0 = \infty$. Since $\rho(0) = 0$ and $\rho(t)$ is a continuous function of time, then $\forall t \in [0, t_0)$, $|\dot{\theta}(t)| < M$. Now, for any $\epsilon \in (0, \frac{\pi}{4})$, set $\hat{t}_2 = \min\{\frac{\epsilon}{M}, t_0\}$. Then $\forall t \in [0, \hat{t}_2]$, $|\theta(t)| < M\hat{t}_2 \leq \epsilon$. Hence, it follows that

$$\begin{bmatrix} v\,\hat{t}_2\,\cos\epsilon \\ 0 \end{bmatrix} \preceq |\mathbf{r}_v(\hat{t}_2)| \preceq \begin{bmatrix} v\,\hat{t}_2 \\ v\,\hat{t}_2\,\sin\epsilon \end{bmatrix}, \tag{B.1}$$

where $|\cdot|$ and $\preceq$ have to be interpreted as componentwise operators (see the dashed region in Figure B.1). By simple geometric arguments it can be shown that (B.1) implies: $v\hat{t}_2 \cos\epsilon \leq \rho(\hat{t}_2) \leq v\hat{t}_2$ and $\pi - 2\epsilon \leq \gamma(\hat{t}_2) \leq \pi + 2\epsilon$. By recalling the definition of ϵ, it follows that $\rho(\hat{t}_2) > 0$ and $\gamma(\hat{t}_2) \in [0, \frac{3}{2}\pi]$, which means $(\rho(\hat{t}_2), \gamma(\hat{t}_2)) \in \bar{\mathcal{D}}$. Therefore, for any initial condition in $\mathcal{B}$, there exists a finite time $\hat{t} \leq \hat{t}_1 + \hat{t}_2$ such that $(\rho(\hat{t}), \gamma(\hat{t})) \in \bar{\mathcal{D}}$. This concludes the proof.

C Proof of Lemma 3

Without loss of generality, let us compute matrix B from the equations

$$\dot{\rho}_2 = -v\,\cos\gamma_2 \tag{C.1}$$

$$\dot{\gamma}_2 = \frac{v}{\rho_2}\,\sin\gamma_2 - u_2 \tag{C.2}$$

$$\dot{\gamma}_{12} = \frac{v}{\rho_{12}}\,(\sin\gamma_{12} + \sin\gamma_{21}) - u_1. \tag{C.3}$$

where

$$\rho_{12} = \rho_1 \cos(\gamma_{12} - \gamma_1) + \sqrt{\rho_2^2 - \rho_1^2 \sin^2(\gamma_{12} - \gamma_1)}, \quad \text{(C.4)}$$

$$\gamma_{21} = \gamma_2 - \arcsin\left(\frac{\rho_1}{\rho_2}\sin(\gamma_{12} - \gamma_1)\right). \quad \text{(C.5)}$$

and $u_1 = f_{1b} = k_b\, g(\rho_1; c_b, \rho_0)\, \gamma_1$; $u_2 = f_{2b} + f_{21} = k_b\, g(\rho_2; c_b, \rho_0)\, \gamma_2 + k_v\, g(\rho_{21}; c_v, d_0)\, \gamma_{21}$. Let us consider the equilibrium (36), $\xi_e \doteq [\rho_e \ \frac{\pi}{2} \ \rho_e \ \frac{\pi}{2} \ \frac{\pi}{2} + \arccos(\frac{d_0}{2\rho_e})]'$. Notice that, by substituting ξ_e into (C.4)-(C.5), one gets $\rho_{12} = d_0$ and $\gamma_{21} = \frac{\pi}{2} - \arccos(\frac{d_0}{2\rho_e})$. By linearizing system (C.1)-(C.3) at the equilibrium ξ_e, one obtains matrix $B = \{b_{ij}\} \in \mathbb{R}^{3\times 3}$ with $b_{11} = b_{13} = b_{33} = 0$, $b_{12} = v$ and

$$b_{21} = \frac{v}{\rho_e^2} + k_b \frac{c_b - 1}{(c_b - 1)\rho_e + \rho_0}\frac{\pi}{2} + k_v \frac{c_v - 1}{c_v d_0}\left(\frac{\pi}{2} - \arccos\left(\frac{d_0}{2\rho_e}\right)\right)\frac{2\rho_e}{d_0}$$

$$b_{31} = \frac{v}{2\rho_e^2}, \quad b_{22} = \frac{2v}{\pi\rho_e}, \quad b_{32} = \frac{v}{d_0}\sqrt{1 - \frac{d_0^2}{4\rho_e^2}}.$$

$$b_{23} = k_v \frac{c_v - 1}{c_v d_0}\sqrt{4\rho_e^2 - d_0^2}\left(\frac{\pi}{2} - \arccos\left(\frac{d_0}{2\rho_e}\right)\right)$$

Now, let us write the characteristic polynomial of B as $P_B(\lambda) = \lambda^3 + a_1\lambda^2 + a_2\lambda + a_3$, where, by trivial calculations, one has $a_1 = b_{22}$, $a_2 = vb_{21} - b_{23}b_{32}$, $a_3 = vb_{31}b_{23}$. The coefficients a_1 and a_3 are trivially positive because $b_{ij} \geq 0\ \forall i, j$. For the term a_2, one can observe that

$$\frac{b_{23}b_{32}}{v} = k_v \frac{c_v - 1}{c_v d_0}\left(\frac{\pi}{2} - \arccos\left(\frac{d_0}{2\rho_e}\right)\right)\left(\frac{2\rho_e}{d_0} - \frac{d_0}{2\rho_e}\right) \leq k_v \frac{c_v - 1}{c_v d_0}\left(\frac{\pi}{2} - \arccos\left(\frac{d_0}{2\rho_e}\right)\right)\frac{2\rho_e}{d_0} \ \leq \ b_{21},$$

which implies positiveness of a_2. Therefore, by applying the Routh-Hurwitz criterion to $P_B(\lambda)$, matrix B turns out to be Hurwitz if $a_1a_2 - a_3 > 0$. Then, one has

$$a_1a_2 - a_3 = b_{22}(vb_{21} - b_{23}b_{32}) - vb_{23}b_{31} = \frac{2v^3}{\pi\rho_e^3} + k_b\frac{c_b - 1}{(c_b - 1)\rho_e + \rho_0}\frac{v^2}{\rho_e} + k_v\frac{c_v - 1}{c_v}\left(\frac{\pi}{2} - \arccos\left(\frac{d_0}{2\rho_e}\right)\right)\frac{v^2}{\rho_e^2}\left(\frac{1}{\pi} - \frac{1}{2d_0}\sqrt{4\rho_e^2 - d_0^2}\right).$$

By letting $\phi = \frac{\pi}{2} - \arccos(\frac{d_0}{2\rho_e})$, one can rewrite the last r.h.s. term of the previous equation as $\frac{1}{2}k_v\frac{c_v - 1}{c_v}\frac{v^2}{\rho_e^2}\, r(\phi)$, where $r(\phi) = \phi(\frac{1}{\pi/2} - \frac{1}{\tan\phi})$. Since $0 \leq \phi \leq \frac{\pi}{2}$, one has that $r(\phi) \geq -1$. Moreover, because $\rho_e > \rho_0$, the following inequality holds

$$a_1a_2 - a_3 > \frac{2v^3}{\pi\rho_e^3} + k_b\frac{c_b - 1}{c_b}\frac{v^2}{\rho_e^2} - \frac{1}{2}k_v\frac{c_v - 1}{c_v}\frac{v^2}{\rho_e^2}. \quad \text{(C.6)}$$

Now, it is easy to see that $\dfrac{k_v}{k_b} \leq 2\,\dfrac{c_v}{c_b}\,\dfrac{c_b - 1}{c_v - 1}$ is a sufficient condition for the right hand side of (C.6) to be positive. This concludes the proof.